UNIVERSIDADE FEDERAL FLUMINENSE

DANIELLE LOPES DA SILVA

FULL WAVEFIELD SIMULATIONS IN ANISOTROPIC MEDIA APPLIED TO THE STUDY OF THE NORTHERN APPALACHIAN ANOMALY

Niterói,
Brazil

2017

DANIELLE LOPES DA SILVA

FULL WAVEFIELD SIMULATIONS IN ANISOTROPIC MEDIA APPLIED TO THE STUDY OF THE NORTHERN APPALACHIAN ANOMALY

Senior thesis presented to the bachelor in geophysics program of the Universidade Federal Fluminense as a requirement for the bachelor degree.

Advisor: William Menke

Universidade Federal Fluminense - UFF

Geology and Geophysics Department

(LAGEMAR)

Bachelor in Geophysics program

Niterói,
Brazil

S586 Silva, Danielle Lopes da

Full wavefield simulations in anisotropic media applied to the study of the Northern Appalachian Anomaly / Danielle Lopes da Silva. — Niterói : [s.n.], 2017.

47 f.

Trabalho de Conclusão de Curso (Bacharelado em Geofísica) – Universidade Federal Fluminense, 2017.

1.Anisotropia sísmica. 2.Anomalia do Norte dos Apalaches. 3.Ondas de cisalhamento. I.Título.

CDD 622.1592

Danielle Lopes da Silva

Full wavefield simulations in anisotropic media applied to the study of the Northern Appalachian Anomaly

Senior thesis presented to the bachelor in geophysics program of the Universidade Federal Fluminense as a requirement for the bachelor degree.

Advisor: William Menke

Aproved in __/__/____

EXAMINERS

_____

Dr. William Menke (Advisor)
Lamont-Doherty Earth Observatory (LDEO)

_____

Dr. Alexandre Motta Borges (co-advisor)
Universidade Federal Fluminense (UFF)/Lagemar

_____

Dr. Luiz Alberto Santos
Universidade Federal Fluminense (UFF)/Lagemar

Niterói,
Brazil

This work is dedicated to all professors working at Lamont-Doherty Earth Observatory that made my summer of 2016 more than special.

ACKNOWLEDGEMENTS

First of all, I would like to thank all the professors from Lamont-Doherty Earth Observatory for the opportunity of learning and having fun with all the other interns. A special thank to Bill, for teaching me about geophysics, for the long talks about my future and for keeping contact, making possible to me to write this work.

I appreciate my co-advisor Alex Motta Borges for his support during my formation in geophysics at UFF and his caring in agreeing being my co-advisor.

I am grateful to CAPES for giving me the opportunity to participate of the Science without Borders program and work at Lamont-Doherty Earth Observatory on the project that inspired this work.

I am also incredibly thankful to the SDB team at ANP. Mainly to André and Morelatto, my internship advisors, for the talks about geophysics, geology, programming, life and memes.

I have to mention here people that were indispensible during the time I studied at UFF. To all my dear friends, thank you very much for helping me, listening, caring and for being there when I needed. Mainly to Clara, Esthephany and Laisa for the long talks, I'm very thankful.

To dear Ana Carolina, who had to deal with me talking, reading and breathing geophysics even though she was not very interested in it, thank you for helping me and caring even when no one else could. You were more patient than I thought you could be. This diploma is yours too.

I also thank my family for all the support I received during my academic formation. Especially to my brother Rafael and my mom for all support, affection, and for always believing that I can achieve everything I desire.

ABSTRACT

The Northern Appalachian Anomaly (NAA) is an unusual low velocity zone located at the eastern edge of the thick, cool and tectonic stable North American craton. Over the past 20 years, several studies about this anomaly came up with different ideas of what it could be. Besides being located in a tectonically stable area, previous studies could not detect any significant change in the asthenosphere thickness caused by the NAA. Based on the idea that this anomaly is caused by the presence of a local mantle upwelling, a simplified anisotropic model of the Earth was built to simulate a shear wave pulse propagating though it. This project uses a preexisting MATLAB script to simulate full wavefield propagation, allowing the test of the hypothesis that wave diffraction masks changes in the mantle anisotropy and make its geographic distribution not easy to correlate to the shear wave velocity anomaly area . A post- processing script, also written in MATLAB, was developed to measure the shear wave splitting and the travel time along an array of 80 stations at the top of the model. As a result, we were able to compare the measurements after simulations with the ones predicted by the ray theory and understand how the wave diffraction phenomenon affects the measurements of shear wave splitting time in a low velocity zone for different sizes of anomaly.

Key words: *Seismic anisotropy, shear wave splitting, Northern Appalachian Anomaly*

LIST OF ILUSTRATIONS

LIST OF EQUATIONS

CONTENTS

1. INTRODUCTION

The Northern Appalachian Anomaly (NAA) is a narrow (~400 km wide) and low velocity anomaly in the upper mantle (100 – 300 km depth) localized in New Hampshire (centered at N42.81, 72.17W). The anomaly is set on the northeastern of United States, in the North American craton, which means the area supposed to have a cold, old and thick lithosphere (Menke *et al*., 2016). Since a such strong seismic anomaly like the NAA is not expected in a tectonic setting like this, studies came up with different explanations for what would produce that in the North American craton surroundings. The first explanation was that the NAA was a consequence of the Great Meteor hotspot that crossed the New England around 100 Ma. However, Li *et al*. (1998), using data from MOMA (Missouri to Massachusetts Broadband Seismometer Experiment), studied the variation of the asthenosphere thickness in the area and were not able to detect significant changes. Besides, according to new tomography data inversion (Menke *et al*., 2016), the NAA is close but not parallel to the hotspot track, which contradicts this idea.

Menke *et al.* (2016) came up with the idea that the NAA was caused by a local convection cell in the mantle. This project is based on this idea and applies a full wavefield simulation to understand better how the wave diffraction affects splitting measurements on the NAA.

2. OBJECTIVES

The Northern Appalachian Anomaly is a low velocity anomaly located in the New England region. This anomaly is characterized as unusual because it is set in a cratonic and tectonically stable area. In an attempt to understand the presence of the anomaly in this area a new explanation came up with the idea that it is caused by a local convection cell in the Earth's mantle.

Shear wave splitting measurements in the region identified a pattern of null splitting time values in the southern New England. This pattern is expected for a mantle cell convection but its location do not correlate with the center of NAA.

This project uses seismic modeling to understand if the wave diffraction phenomenon is able to affect the shear wave splitting measurements made by previous studies.

The main objectives of this work are listed in the following items:

I. To build a simplified model of the NAA using MATLAB.

II. Simulate a full wavefield propagation through the model using the wave algorithm.

III. To record shear wave splitting and travel time measurements based on the seismograms computed after the simulation.

IV. To compare results after measurements with expected results predicted based on the ray theory for different widths of anomaly.

3. AREA OF STUDY

3.1. The Northern Appalachian Anomaly

New England is a region of the northeastern United States that includes the states of Vermont, Connecticut, Massachusetts, New Hampshire, Maine and Rhode Island. The Appalachian mountain range is one of the important features that characterize the relief of the area and it extends from Alabama to the state of Maine (Figure 1).

The Grenville belt is set in the eastern hemisphere of the United States and its origin is associated with the Grenville orogen whose formation is dated to approximately 1100 million years and was caused by the collision of the continent Laurentia with another continent, which is believed to be the Amazon. The metamorphism process in the Grenville orogen began about 1090-1020 Ma, then migrated so that the most recent deformations are in the northeastern area and dated to 1000-980 Ma (Hynes & Rivers, 2010).

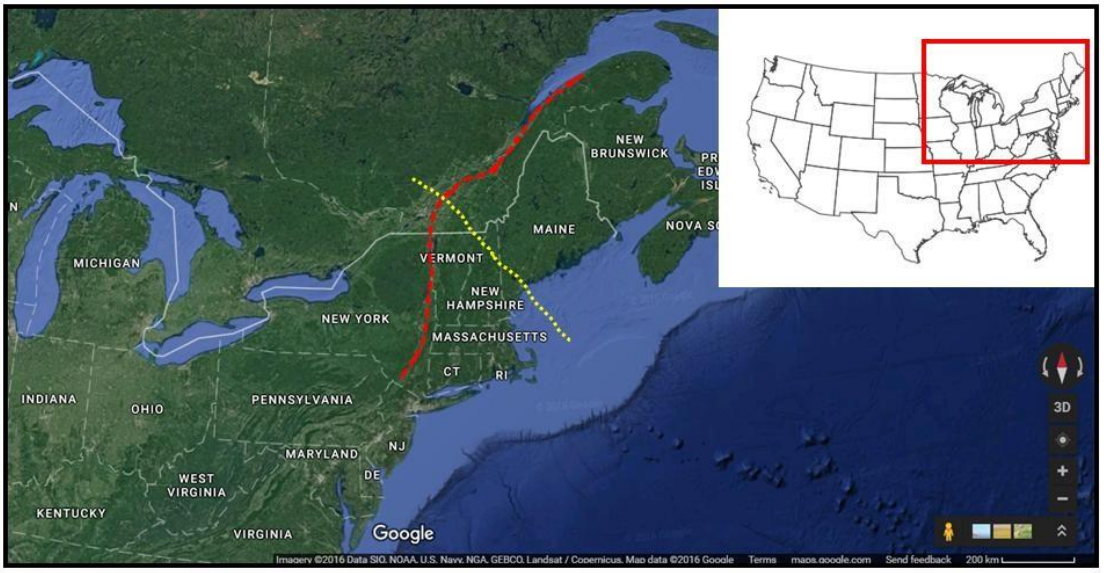

Figure 1:Area of study and states in New England (Vermont, Connecticut, Massachusetts, Nova Hampshire, Maine e Rhode Island). The Appalaches mountain is presented by the dashed and red line whereas the yellow line is the track of the Great Meteor hotspot.

The ~400 Ma Appalachian orogeny, located to the east of the Grenville belt, is directly associated with the formation of the Pangea supercontinent and the sediments from the erosion that operates in the mountain range extend in the regions from east and west of it. The height of the orogen has already reached similar elevations to the Alps and the Rocky Mountains in the western of the United States (Bartholomew & Whitaker, 2010). The Appalachian mountain delimitates the western part of the NAA and the eastern of the North American craton.

Seismic tomography is the technique that uses measurements of the travel time of compressional and shear waves produced by earthquakes from distant areas to image the Earth. The location and size of the time anomalies will depend on the lateral velocity variation and slowness of the waves that are traveling in the subsurface (Waldhauser *et al.*, 2002).

The eastern part of the North American continent is marked by significant variations in the velocity of seismic waves (Levin *et al.*, 1995) such as the Central Appalachian anomaly (CAA) and the Northern Appalachian Anomaly (NAA). The NAA is a strong low velocity anomaly located in the upper mantle of the New England region centered at 42.81 ° N, 72.17 ° W, in New Hampshire. The initial explanation for the existence of a seismic anomaly such as the NAA in a tectonically stable region like this is that the NAA had been originated from the Great Meteor Hotspot (Figure 1), which crossed the area about 100 million years ago (van der Lee And Nolet, 1997, Eaton and Frederiksen, 2007). Menke *et al.* (2016) came up with the hypothesis that the NAA is a modern feature associated with a small-scale asthenospheric upwelling that is not related to any hotspot. Results of the work developed in Menke *et al.* (2016) show that the NAA is about 400 km wide and it is located between 100 and 300 km deep.

Seismic tomography studies in the New England region show that the seismic anomaly produced by the NAA corresponds to a variation of 700 ° C in the upper mantle which inspires the idea that the NAA is a modern and thermal anomaly possibly caused by the rise of the Earth's mantle (Menke *et al.*, 2016). In addition, tomographic travel time inversion, measured for both compression and shear waves, produced velocity maps for different depths in the New England area, identifying that the anomaly becomes wider with depth and is not parallel to the hotspot track. Figure 2 shows results of the seismic imaging done in the New England region showing NAA at different depths (100, 200 and 300 km).

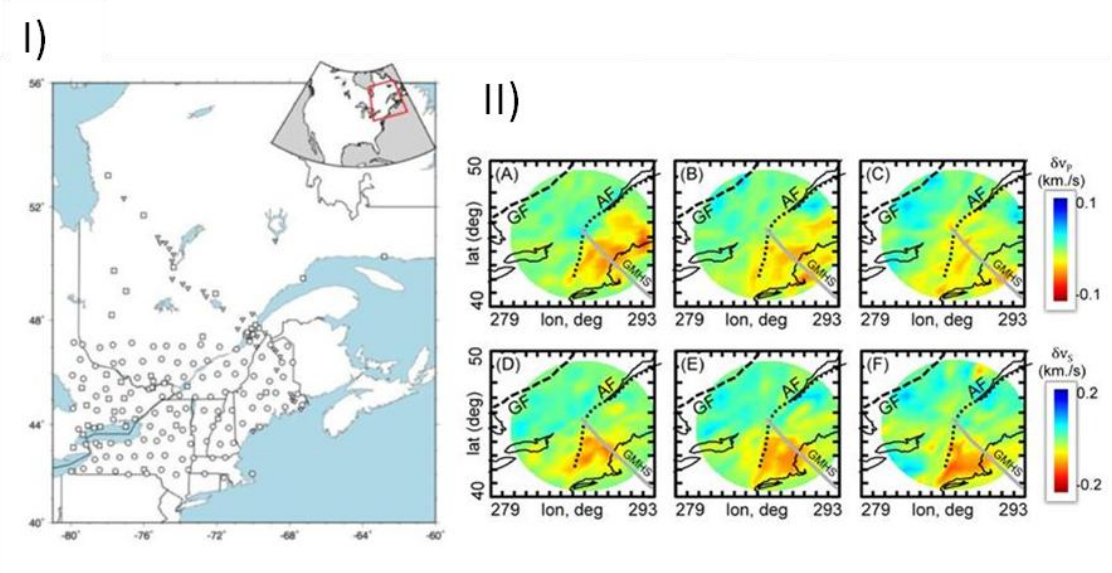

Figure 2: Part I of the figure shows the stations used for the tomographic study. It includes permanent stations (squares), Earthscope 141 Transportable Array stations (circles) and Earthscope Flexible Array QMIII stations (triangles). Part II shows the Appalachian Front (AF), Grenville Front (GF) and Great Meteor Hotspot (GMHS) track in the compressional wave and shear wave pertubations for 100, 200 and 300 km. A, B and C are the tomographic maps for the P wave velocity whereas the maps D, E and F are the maps for the S wave velocity (Menke et al., 2016).

Using data from teleseismic arrivals, Long *et al.* (2006) were able to calculate the shear wave splitting time distribution in the northeastern United States. The Figure 3 represents this distribution that was found using the seismic stations in the area (red and white circles). The black bars in the map represent the amount of splitting measured by each station whereas the orientation of the bars represent the direction of propagation for fast

shear waves. The stations with no bars over them are the ones that detected null shear wave splitting measurements ("null measurements"). There are several stations like that in the map, which is what it would be expected in a mantle convection area. However, the local distribution of the "null measurements" do not correlate with the center of the shear wave anomaly. The geometry of the "null measurements" is more complex and located in the southern area. This work tries to understand if the wave diffraction phenomena can affect the shear wave splitting measurements in order to change its shape and amplitude.

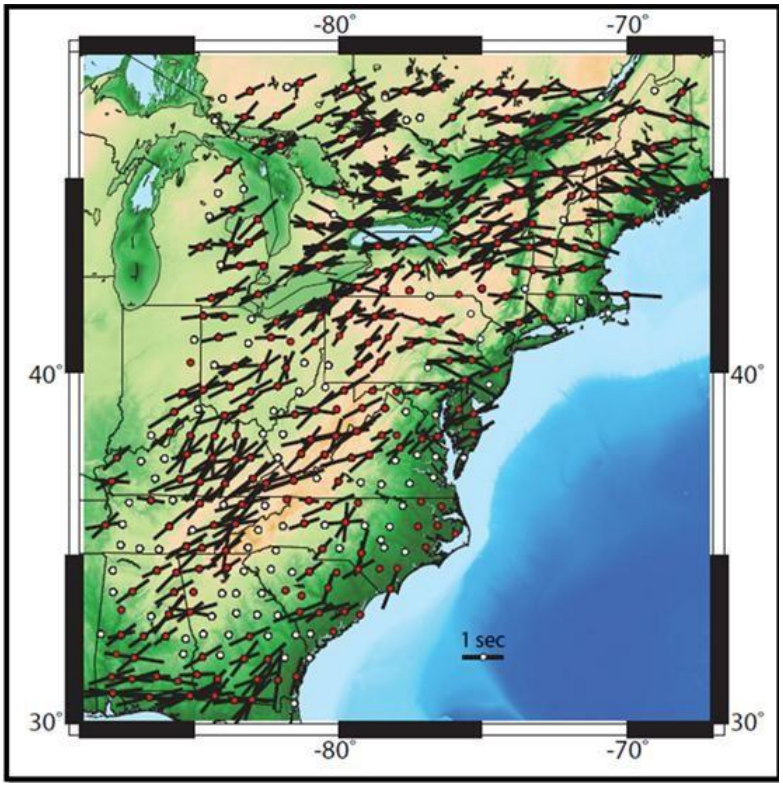

Figure 3: Results of shear wave splitting analysis in the northern United States. Each point in the map represents a seismic station that was used in the study and the length of the bars means the amount of splitting (that will be better explained in the next sections) measured in the station. If the splitting measured is big it means that the anisotropy in the area is high. The direction of the bars represents the direction in which the shear wave propagates faster. The white circles represent stations where were detected null splitting measurements in at least five shear waves arrivals. In the southern part of the figure (where the NAA is) there are several stations that were not able to detect splitting (Long, 2016).

3.2. Edge-driven Convection

The results of tomography data inversion and previous studies like the one from Long (2016), reinforce the description of NAA from Menke *et al.* (2016). The Figure 4

illustrates the interpretation of NAA by Menke *et al.* (2016) which is inspired by the convective model described in King and Ritsema (2000).

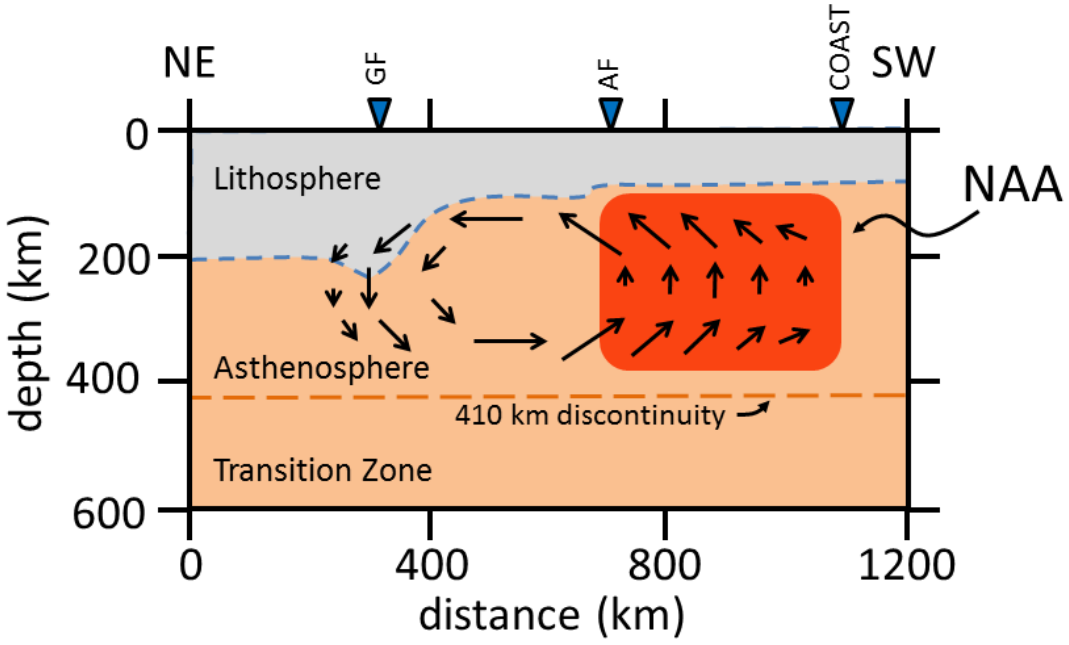

Figure 4: Northern Appalachian anomaly model based on the Edge-Driven Convection model. It shows the difference of lithosphere thickness that yields an instability in the asthenosphere, and generates a small-scale convection in the asthenosphere (Menke *et al.*, 2016).

The model described by King and Ritsema (2000) is called Edge-driven convection (EDC). In simple words, they believe that the difference of lithosphere thickness can cause small-scale convections in the asthenosphere. The edge in the lithosphere would create strong lateral temperature and viscosity contrasts and induce a small-scale form of convective flow in the mantle beneath the craton margin in its transition with a thin oceanic lithosphere. The EDC model is able to explain the location of intraplate volcanos on the African and South American plates and the seismic wave velocity anomalies in cratonic lithosphere.

4. LITERATURE REVIEW

4.1. Theory of seismology

Seismology is the main geophysical method used for the study of Earth's structure and composition. It is also related to the study of physical processes that cause earthquakes and the planning to minimize their destructive impacts (Shearer, 2009)

Lay (1995) described seismology as the study of the generation, propagation, and recording of elastic waves on Earth and the sources that produce them. Both active (human-generated) and passive (or natural, which is the focus of this work) sources are capable of generating seismic waves and elastic disturbances that expand spherically from the source and propagate through the Earth. The propagation of these waves is described by several physical principles that will be discussed in this section.

Earthquakes are mechanical vibrations resulting from the elastic behavior of the Earth, which provides the excitation and propagation of elastic waves through it (Lay, 1995). These waves generate disturbances that can be recorded by seismometers in order to be analyzed for scientists later. Earthquakes radiate seismic waves traveling the Earth causing disturbances that can be detected by seismometers anywhere in the globe.

Seismograms are records of the displacement of the ground caused by the waves as a function of time. They are also the main tool used by seismologists in the study of elastic waves and the Earth's structure (Lay, 1995).

Since different types of seismic waves have distinct velocities in a medium, seismologists are able to identify them in a seismogram observing their respective arrival times. P, S, Love and Rayleigh waves have different characteristics. Poisson, in 1830, used wave

propagation equations to prove that two types of wave propagate within homogeneous solids: P waves and S waves (Figure 5). P waves are compressional waves that cause volumetric perturbations in the particles, disturbing them in the direction of propagation, such as sound waves. S waves do not cause change in the volume of the particles, however they have a shearing characteristic, disturbing the particles transversely to the direction of propagation and are not able to propagate in fluids.

The P (primary) wave is also faster than the S (secondary) wave (Lay, 1995).

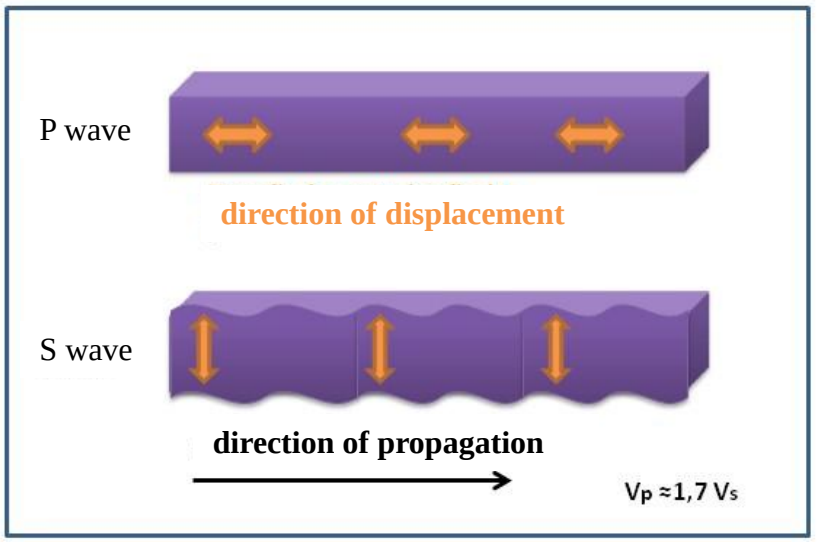

Figure 5: P and S waves propagating through a medium. The yellow arrows represent the direction of displacement of the particles and the black arrow is the direction of propagation. The shear wave disturbs the particles in the direction orthogonal to the direction of propagation whereas the P wave disturbs the particles in a direction parallel to the direction of propagation. The velocity of the P wave is also bigger than the S wave in a scale factor of 1.7.

One of the main applications of seismology is the study of the Earth's structure and the physical processes that affect it. Most of the knowledge about the interior of the Earth such as, its structure, composition, dynamics, physical processes and temperature has been based on seismological observations. Pioneers in the field, such as Jeffreys, Bullen, Gutemberg, and Lehmann, have come to results that are fundamentally important nowadays, such as the existence of a fluid core since the S wave cannot propagate through it (Lay, 1995).

The velocity of propagation of seismic waves depends on physical properties of the medium, such as density (**ρ**) and the elastic moduli. Elastic moduli are ratios that quantify and describe the behavior of the medium undergoing deformation. Among them, the shear modulus or stiffness (**μ**) and the volumetric modulus (***k***) stand out. The stiffness modulus is defined as the ratio between the shear strain that a body undergoes and the stress responsible for the deformation. The volumetric modulus is defined as the ratio of the volumetric strain suffered by the body and the stress applied on it.

P wave (V_p) and S wave (V_s) velocities are mathematically described in function of these moduli as:

$$V_p = \sqrt{\frac{\frac{3}{4}\mu + k}{\rho}}, \qquad Eq.1$$

$$V_s = \sqrt{\frac{\mu}{\rho}}. \qquad Eq.2$$

Temperature is one of the factors that influence the velocity of propagation of seismic waves in the interior of the Earth. One hundred degrees Celsius of contrast in the mantle temperature would produce a change of about 1% in the speed of the seismic waves (Lay, 1995). This difference in temperature would also be enough to generate a process of flow and convection at large scales. Figure 6 shows a map for shear and compressional waves velocities anomalies distribution in United Stated for 75 km and 200 km depth. The red areas represent low velocity zones and can be related to hotter lithosphere and asthenosphere whereas the blue areas are related to cold and stable areas. Most of those thermal anomalies are related to tectonic activity such as the western United States active margin. The seismic anomalies in eastern United States, such as NAA (Northern

Appalachian Anomaly) and CAA (Central Appalachian Anomaly) cannot be related to tectonic activity but could be explained by the edge-driven convection model.

To obtain truly valuable information about the Earth's structure with a reasonable level of confidence and resolution, a collection with a large number of seismological observations at different distances from the seismic source is required. Since the internal structure is divided into layers, all of these layers is capable of generating reflections and variations of P and S waves travel times. The amount of time that a seismic wave takes to propagate from the source to the seismometers determines the structure, its discontinuities and the speed of the Earth's interior (Lay, 1995).

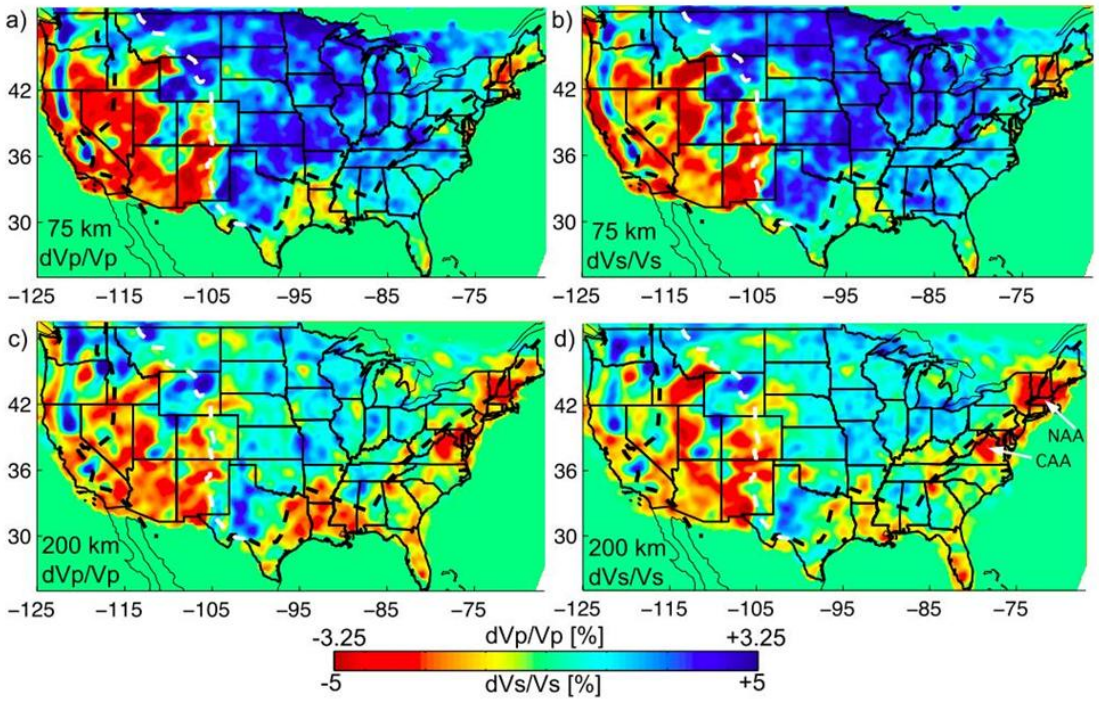

Figure 6: Velocity anomalies distribution map in the USA for compressional and shear waves in 75 km and 200 km of depth. The red areas are related to low velocity zones and many times to hotter areas. The American active margin is in the west of the map whereas the central of the country is dominated for a stable and cold lithosphere. The American passive margin is in the east of the map, however there are some low velocity anomalies that are not related to tectonic activity but possibly to the presence of mantle uppwelling caused by the process of edge-driven convection (Schmandt & Lin, 2014).

4.1.1 Stress and strain

Seismology is related to elastic disturbances, which means that seismic waves deform the Earth in an ephemeral way, causing the material to return to its original position after the force is no longer being applied. The recorded disturbances are related to vibrations that involve small elastic strains in the rocks caused by the internal forces (stress) applied on them. Since these deformations are considered elastic, there is a vast mathematical theory capable of reasonably describing these events and the stress / strain relationship in a material as the wave propagates through it. The purpose in this section is to present this theory. In most cases, seismology is the study of relatively small deformations with infinitesimal perturbations (relative changes in length on the order of 10^{-6} m) in short periods of time (<3600 s). This mathematical description is called the infinitesimal strain theory and it makes possible for the mathematical description of events to be simple (Lay, 1995). The relationship between strain and applied stress on a material (in the infinitesimal strain case) is described by Hooke's law: $F = K(l_1 - l_0)$.

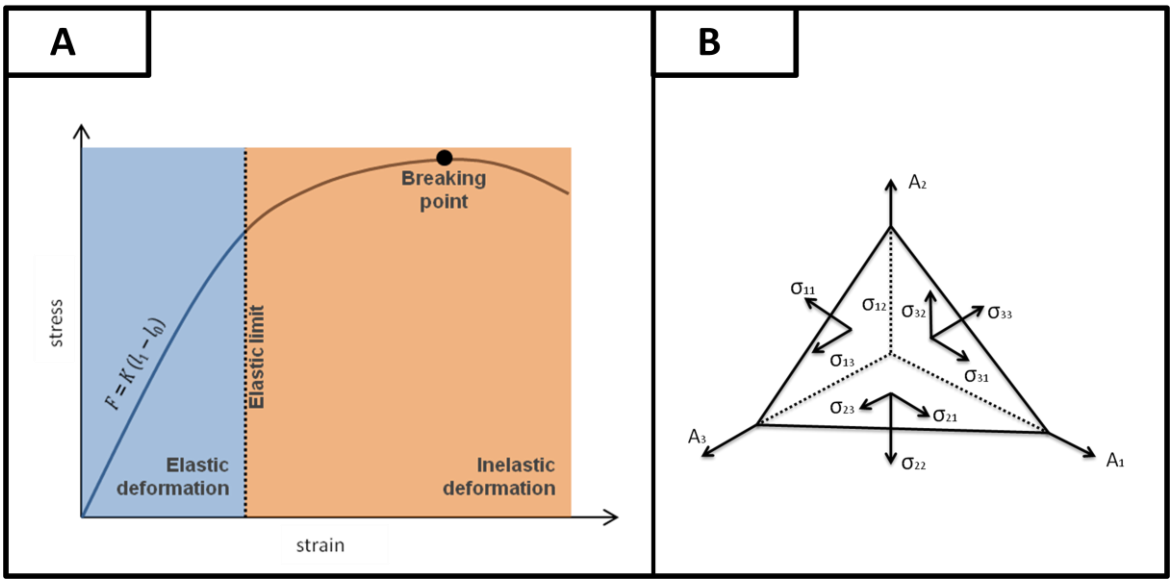

Figure 7: (3a) Graph of the relationship between stress and strain in an elastic and inelastic deformation. In the elastic situation the relationship is described by a straight line (Hooke's law). (3b) Three orthogonal plans in the space and the forces parallel and orthogonal to them that are able to describe any force acting on any point of the space (modified from Lay, 1995).

Hooke's law describes these deformations as a function of the properties of the material such as its density, stiffness (resistance that the material presents when a shearing stress is applied) and its compressibility (resistance that the material presents to the change in its volume). Figure 7a shows a graph of the relationship between stress and strain for elastic and inelastic deformations. Once the deformation on the material becomes inelastic, Hooke's law is no longer able to describe the phenomenon suffered by the body (Lay, 1995).

As already mentioned, in order to elastically deform a body it is necessary to apply a force on it. There are two types of force that can act on a body: Body forces and contact forces. Body forces affect the volume of the material and are proportional to properties such as density. An example of body force is the gravity, where the modulus of the force depends on the mass of the material and the acceleration of gravity. Contact forces depend on the contact area of the material, such as the frictional force and the resistance force of the air.

In order to define the applied forces in a body, it is necessary to think of three orthogonal planes defined by three different directions. The surfaces are called surfaces 1,2 and 3. In order to describe the forces acting on the points of a body, σ_{ij} is defined. Where i corresponds to the direction from normal to the plane where the force is being applied and j corresponds to the direction of force. Figure 7b shows the distribution of these forces being applied on the three orthogonal planes in space.

Thus σ_{11}, σ_{22} and σ_{33} are forces acting perpendicularly to the respective planes, whereas, σ_{12}, σ_{13} e σ_{21}, for example, are forces acting parallel to the planes. All nine combinations of forces acting on the three planes are necessary to describe the complete distribution of forces acting at a point in space. For a body in equilibrium the sum of

these forces must be equal to zero. Lay (1995) shows that the nine components mentioned in the previous paragraph combined linearly are capable of representing stress on any surface of the medium. Thus, the stress tensor is defined by

$$\sigma_{ij} = \begin{pmatrix} \sigma_{11} & \sigma_{12} & \sigma_{13} \\ \sigma_{21} & \sigma_{22} & \sigma_{23} \\ \sigma_{31} & \sigma_{32} & \sigma_{33} \end{pmatrix}. \qquad Eq.3$$

The terms on the diagonal of the matrix are called normal stresses whereas the others are called shear stresses.

The tensor of elasticity, c_{ijkl}, is a four-dimensional matrix with 81 components (3^4) that quantifies the stress caused by an applied strain (Shearer, 2009). However, due to symmetry in the operator, only 21 elements are independent for elastic media. These 21 elements specify the ratio of stress to strain for an elastic solid. The tensor can be written as

$$c_{ijkl} = \lambda\delta_{ij}\delta_{kl} + \mu\left(\delta_{il}\delta_{kj} + \delta_{ik}\delta_{jl}\right), \qquad Eq.4$$

where λ and μ are the Lamé parameters of the material and the δ is the Kronecker delta (δ_{ij} =1, when i=j e δ_{ij} =0, when i≠j).

The second parameter of Lamé has already been described in this text as a shear modulus or stiffness modulus. The first parameter in turn can be written as a function of the velocities of the seismic waves as

$$\lambda = \rho\left(V_p^2 + V_s^2\right). \qquad Eq.5$$

4.1.2. Ray theory

Ray tracing is a simplified and convenient way of representing wave propagation, in which it is possible to extend the elastic solutions of propagation in homogeneous media to non-homogeneous media in an intuitive way. This approximation is known as geometric ray theory and is fundamental understanding the interpretation of body wave propagation (Lay, 1995). Wave rays are always perpendicular to the wave fronts as they propagate. For a plane wave the rays will be straight lines parallel to each other and for spherical waves they are radial lines that get together in the source point.

One of the fundamental concepts to understand the theory of classical optics is the Huygens principle, which starts from the idea that each wavefront point can be considered a seismic source.

The principle that is crucial in the geometry of the rays is called principle of Fermat. The principle is based on the idea that the waves will always go through the path that will make it take a shorter time to propagate.

These principles greatly simplify the mathematical and consequently computational description of the seismic waves propagation. Because of their simplicity and applicability to a variety of problems, the approximations continue to be used extensively. These applications include most earthquake localization algorithms, body wave focus determination algorithms, and inversions for velocity distribution in the mantle and the earth's crust. These simplifications are relatively easy to understand and apply but have significant limitations. They are not able to predict any non-geometric effect, such as head waves or the diffraction (Shearer, 2009).

4.1.3. Shear wave splitting analysis

The study of the Earth's structure and the physical phenomena that affect the crust and mantle are important areas in geology. However, for a long time the focus of geology was to understand the processes that affect the crust. With the advent of plate tectonics, geology became wider and now the crust is considered to be a small part of a much larger and more dynamic system, in which the mantle plays an important role in driving crust deformation. Plate tectonics explained the formation of orogen areas as being the result of collisions between tectonic plates predicted in the Wilson's cycle (Silver, 1996). The advent of the theory associated the interaction between plates, the deformation within them and their coupling were associated with the dynamics of the mantle below them, generating great interest for this component in the structure of the Earth.

The purpose of this section is to present the shear wave splitting analysis. However, in order to understand this, it is necessary to introduce the concept of seismic anisotropy. Silver (1996) describes seismic anisotropy as the property of a material that generates variations in velocity as a function of propagation and direction of polarization of seismic waves.

The study and use of anisotropy in the mantle as a form of measurement can provide valuable information about the Earth's structure, however it requires knowledge from different techniques as well. The factors that can cause seismic anisotropy are: layering of isotropic materials with different elastic properties (Backus, 1962); Fluid-filled fractures (i.e., Crampin & Booth, 1985; Savage *et al.*, 1989; Kaneshima *et al.*, 1988; Kaneshima & Ando, 1989; McNamara & Owens, 1993; McNamara, 1990); Orientation of anisotropic minerals in the mantle; Or more generally, the deformation of materials (Christensen,

1984, Nicolas& Christensen, 1987). Silver (1996) shows that the seismic anomalies under the crust are dominantly produced by the deformations in the mantle that are related to the formation of orogens on the surface. Consequently the mantle is capable of "fossilize" ancient orogen regions no longer present in the crust.

The anisotropy in the mantle is, most times, concentrated in the upper mantle, composed mainly of olivine, which is anisotropic due to its structure with preferential directions of deformation (Nicolas & Christensen, 1987; McKenzie, 1979; Ribe, 1989a, b; Ribe&Yu, 1991). The wave polarization is capable of generating a discrepancy in the velocity of the shear waves that propagate in different directions. The study of shear wave splitting provides a number of unique information and data set and has been used to map regional variations of transverse anisotropy (eg Schlue&Knopoff, 1977; Nataf *et al.*, 1984; Gaherty&Jordan, 1995).

To understand the propagation of a shear wave in anisotropic media is a fundamental task in order to study the methods used in this project. When a shear wave propagates through anisotropic media, it will be split in two different directions perpendicular to each other (Figure 8). The wave will propagate faster in one direction (fast direction) and it will propagate slower in the other one (slow direction).

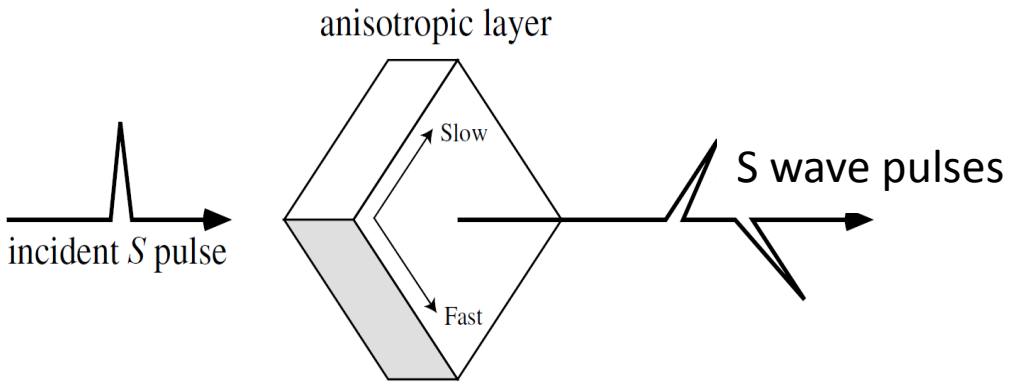

Figure 8: Behavior of a shear wave while it is propagating through a anisotropic media. The wave will be split into two components with different velocities and orthogonal directions (modified from Shearer, 2009).

The difference of velocity between the slow and fast directions of the shear wave will generate a discrepancy in the time they will take to propagate through a medium. This discrepancy is called splitting. If the splitting is longer than the original wavelength, it will be possible to observe two distinct arrivals in the seismogram. For S waves crossing the upper mantle, the time difference between the arrivals of the two pulses varies from 1 to 2 seconds (Shearer, 2009).

There are two different types of seismic anisotropy. The polarization anisotropy and the propagation anisotropy. Propagation anisotropy can be detected by comparing seismic waves that propagate through different paths in the medium. However, most media already have isotropic structural tendencies that also produce distinct seismic wave paths. The propagation anisotropy is considered efficient when applied in the study of the mantle below the oceanic basins. To interpret the polarization anisotropy records is a simpler process than to interpret propagation anisotropy records (Silver, 1996). The type of phenomenon that is expected to be observed in this project is the polarization anisotropy.

One of the most important concepts to understand the data set of shear wave splitting analysis is the idea of shear waves generated by teleseismic tomography, known as S and SKS waves (Figure 9). Teleseismic tomography is a seismic imaging technique that uses records of earthquakes generated at great distances from the seismometers that recorded them. The teleseismic data set has low frequency and an nearly vertical angle of incidence, which makes the technique not efficient on imaging structures in the crust scale. In a seismogram it is possible to identify two different types of shear wave. The S wave and the SKS wave, which is the S wave that is converted into a P wave at the core-mantle boundary (CMB), propagates through the fluid core and is transmitted as a shear wave

again when it returns to propagate in the mantle, being recorded by the seismogram as it reaches the surface.

In most cases, even in an anisotropic medium, the P and S waves will disturb the particles in directions nearly parallel and perpendicular to the direction of propagation, respectively. In an anisotropic medium three types of wave can be observed. The compressional wave P, and two types of wave S. The two components of the S wave will disturb the particles in directions orthogonal to each other and will propagate in different velocities (Silver, 1996).

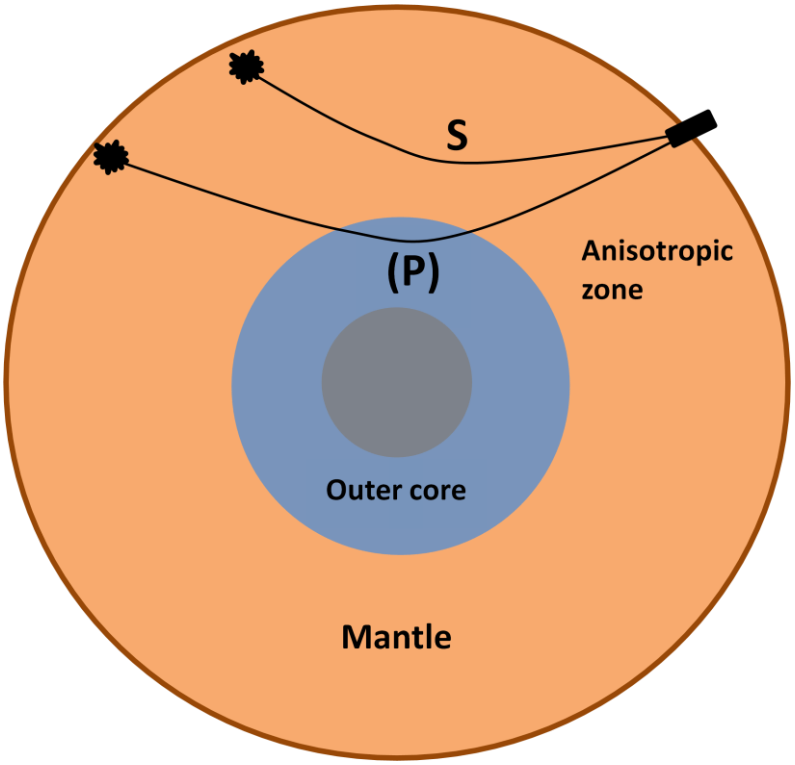

Figure 9: Scheme of the structure of the Earth and the S waves being converted to transmitted SKS waves and P waves when it goes though the fluid outer core.

5. METHODOLOGY

In the section 3.1, results of tomographic studies on the NAA were presented, which characterized it as a seismic anomaly when compared to the surrounding areas. In the same section the interpretation of Menke *et al.* (2016) for this anomaly was presented, in which the NAA is described as a local convection cell in the mantle.

In the section 4.1.3, we discussed the basic aspects and applications of the shear wave splitting technique. In the same section we defined the term splitting as the time difference in seconds between the two components of the shear wave when they propagate in an anisotropic medium.

The mantle convection phenomenon is a strong influence in seismic anisotropy and it can be imagined as a model in which the fast direction of propagation is always parallel to the flow lines. As an anisotropic medium, the mantle causes the shear waves to split into two different components at distinct speeds, causing the seismic stations to record different travel times for each one. The purpose of this work is to use a MATLAB script to simulate a full wavefield propagating in an anisotropic medium such as the NAA and to estimate the arrival times of the S wave and the splitting in time between those components for each station set along the Earth model.

5.1. Earth Model

The advance in computational techniques in the last few years made possible the calculation of robust simulations such as the one used in this project. Boyd (2006) has created a second-order finite-difference code for an anisotropic and elastic wave

simulation in 3D, written in MATLAB based on the idea of a full wavefield, not on the ray theory concepts. The elastic tensor has to be defined for each node in the 3D space. The source set for the simulation is a Gaussian pulse at the bottom of the model.

The script developed by Boyd is composed by two main parts: The first part is responsible for creating a model, defining the necessary parameters to simulate the propagation of the shear wave and defining the seismic source that will generate the wave. The second part of the script is responsible for calculating the three components of the displacement caused by the propagation of the wave at each point in space and for each step in time defined in the first part of the code. The model created in the first part is built based on elastic tensors.

The elastic tensor matrix must be defined for each point in the 2D model. The source was set as a Gaussian pulse that originates from the base of the model. The code allows the user to have several options to build the model: P wave, radial shear wave or a transverse shear wave; to choose between isotropic or anisotropic medium; to choose between elastic or inelastic medium; and to set the number of nodes in the 3 spatial directions. The Earth model that will be used in this project is a 2D simplification of the Menke e al.'s interpretation of the NAA shown in Figure 4. In order to construct this model, three different elastic tensors were necessary, all of them assume that the upper mantle consists of pure olivine.

Figure 10 illustrates how the anisotropy in the olivine crystals affects splitting measurements. The orthorhombic symmetry used makes the calculations easier because the elasticity tensor for them has only 9 independent terms.

The a-axis is depicted as horizontal, so this case corresponds to horizontal mantle flow. The SKS wave propagates vertically, parallel to the b-axis. The two Vs velocities of 4688 and 4254 km/s are very different

along this axis, so the SKS wave experiences a significant amount of splitting. If, on the other hand, the olivine crystal were to be rotated so that its a-axis was vertical (corresponding to mantle upwelling), then the SKS wave would be propagating along the a-axis. The two Vs velocities of 4688 and 4678 km/s are very similar along this axis, so the SKS wave experiences little splitting. Thus, the presence or absence of strong SKS splitting can be used to test whether the mantle is flowing horizontally or upwelling.

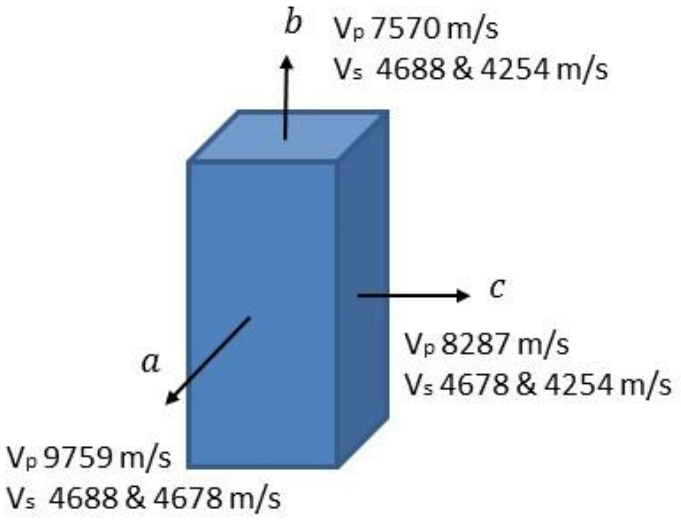

Figure 10: Scheme of a orthorhombic olivine cristal and its anisotropy. The natural anisotropy in the cristal makes the S wave propagate in different velocities in function of the direction of propagation. The level of anisotropy also varies with the direction. The values of velocities are the ones from in the elastic tensor used in the project.

The first one represents an isotropic media, in which the velocities for all the directions of propagation will be the same; the second one is a orthorhombic tensor for a media in which the horizontal direction is the fast axis; and the third one is an orthorhombic tensor for a media in which the vertical direction z is the fast axis. A linear combination of these three

tensors was used in a way that the fast direction axis is nearly parallel to the flow lines that represent the mantle upwelling.

The level of anisotropy was adjusted so that the maximum splitting between the vertical and horizontal displacement component was one second per 100 km of propagation. The width and height of the velocity anomaly was adjusted with a Gaussian curve, where its dimensions in the x and z directions are determined by the standard deviation σ_x and, σ_z respectively, values.

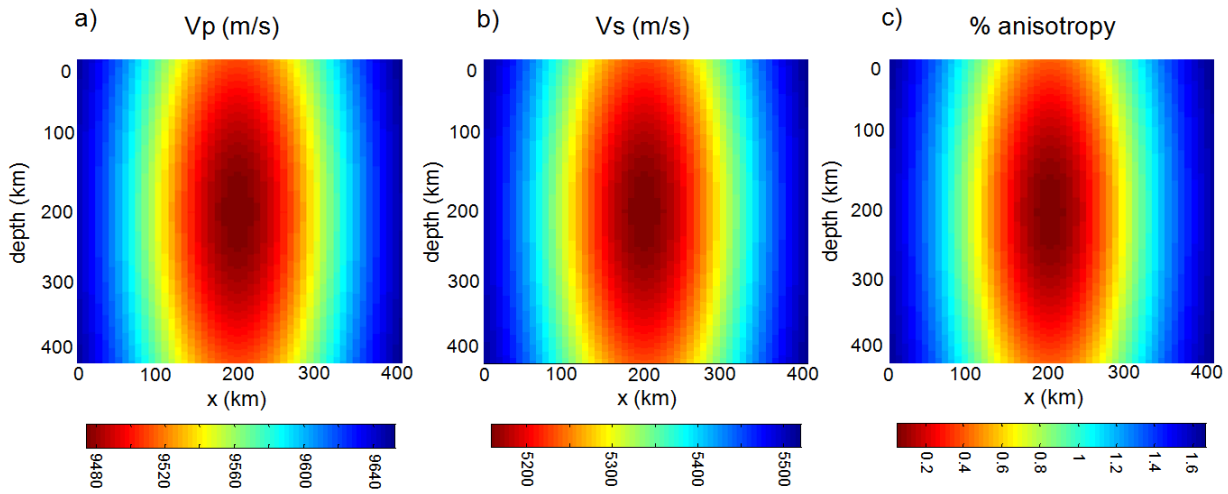

Figure 11: NAA simplification velocity model for compressional (a) and shear waves (b). The shear wave velocity model was calculated using the mean of slow shear wave and fast shear wave velocities. In the right there is the percentage of anisotropy in the model (c).

Figure 11 shows the resulting velocity model for compressional waves, the both shear waves (slow and fast) and the percentage of anisotropy. Both the region of the seismic anomaly such as its surroundings are anisotropic. However, for the case of vertical incidence that is considered in this work only the surrounding areas have significant splitting values.

The algorithms developed in this project were implemented for a rectangular model (400 km by 400 km) and for a source with period pulse of 4 seconds. The computational processes were run for a 100 km wide model and 100 km high and a period source of 1 second to make the process faster, since the linearity of the wave equation allows these simplifications. In order to compute the splitting between the horizontal and vertical components of the seismograms, 80 stations separated by 5 km each were distributed along the top of the model (Figure 12).

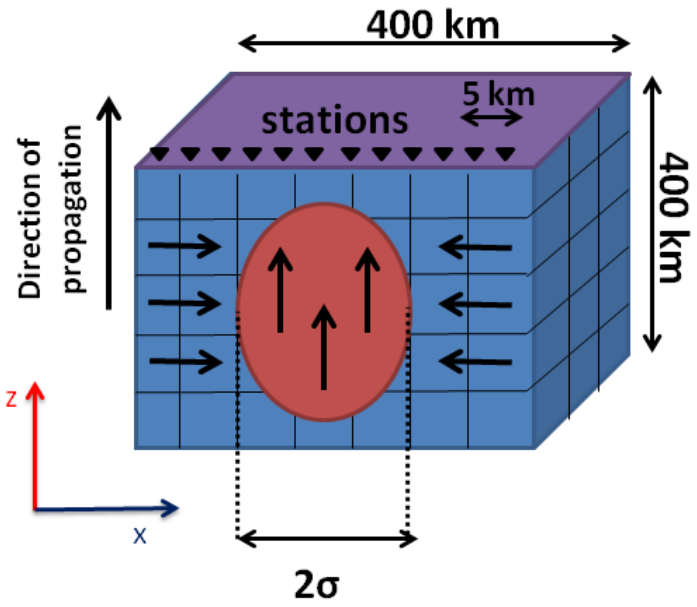

Figure 12: Scheme of the Earth model built on MATLAB. The directions z and x are indicated such as the direction of propagation of the shear wave. The 80 stations are set in the top of the Earth model and will be responsible for recording the displacement of the particles in the x and z directions.

5.2. Full wavefield simulation

The second part of the code is responsible for the wave propagation simulation. In this part, the three components of the displacement caused by the wave are calculated for each point in space and for each moment of the time defined in the first part of the code. The number of loops was minimized making the solution efficient and able to interact with the

user temporally and spatially (it can compute 60000 nodes per second in each times step). The solution derives from tracking the acceleration of a particle, its position and forces action on the mass (Shearer, 1999). Boyd (2006) verified this solution comparing the results with analytical and solution for simple cases and the code was able to successfully discriminate among possible isotropic structures in receiver functions.

The code calculates the solution of the seismic wave equation

$$\rho \frac{\partial^2 \mu_i}{\partial t^2} = \sum_{j=1,3} \frac{\partial \tau_{ij}}{\partial x_j} + f_i \,, \qquad Eq.6$$

where $\boldsymbol{u}$ is the displacement of the particle, $\boldsymbol{x}$ is the spatial component, $\boldsymbol{t}$ is time, $\boldsymbol{\rho}$ the density, $\boldsymbol{\tau}$ the tangential stresses action on the mass and $\boldsymbol{f}$ the forces action on the mass.

In anisotropic media $\boldsymbol{\tau}$ can be written as a function of the elasticity tensor c_{ijkl} as

$$\tau_{ij} = c_{ijkl} \frac{1}{2} (\partial_l u_k + \partial_k u_l). \qquad Eq.7$$

The solution for this equation is based on second-order finite differences approximations where the derivatives are equal to

$$\frac{\partial u}{\partial x} = \frac{u_{i+1} - u_{i-1}}{2dx} \qquad Eq.8$$

and

$$\frac{\partial^2 u}{\partial x^2} = \frac{u_{i+1} - 2u_i + u_{i-1}}{2dx^2}. \qquad Eq.9$$

5.3. Splitting Time Measurements

The following process was applied for each station along the model: The seismograms for the horizontal and vertical components were calculated by the script and computed in different variables. A code was developed that compares the two components and calculates

the splitting between the seismograms using the cross-correlation between them. The code also performs the process of finding the fast direction, choosing the direction that maximizes the cross correlation between the rotated seismograms. This means that the code uses n predetermined angles by the user, rotates the seismograms for each angle and computes the cross correlation between them n times. The angle that makes the cross-correlation reach its maximum value is the angle of the fast direction. Splitting is the time difference necessary to make the two seismograms to align. The code also calculates how the travel time of the two components of the S wave vary along the stations. Each seismogram will be compared with a fixed seismogram (in this case, the first one using the cross-correlation function.) The time needed to align them represents the difference in travel time along the model.

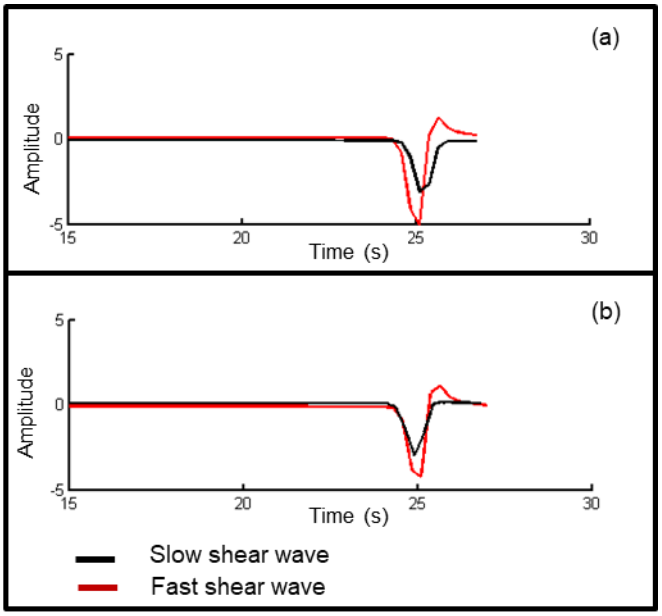

Figure 13: Slow and fast shear waves(black and red) identified by station 40 before and after splitting time correction.

6. RESULTS

This section presents the results obtained from the processes described in the previous section. First of all, after the implementation of the full waveform simulation (described in section 5.2**)** in the NAA simplification model (described in 5.1) it was possible to see how the seismic waves behave when they travel through a low velocity anomaly area. Figure 14 shows the displacement of the particles in the model for directions X,Y and Z.

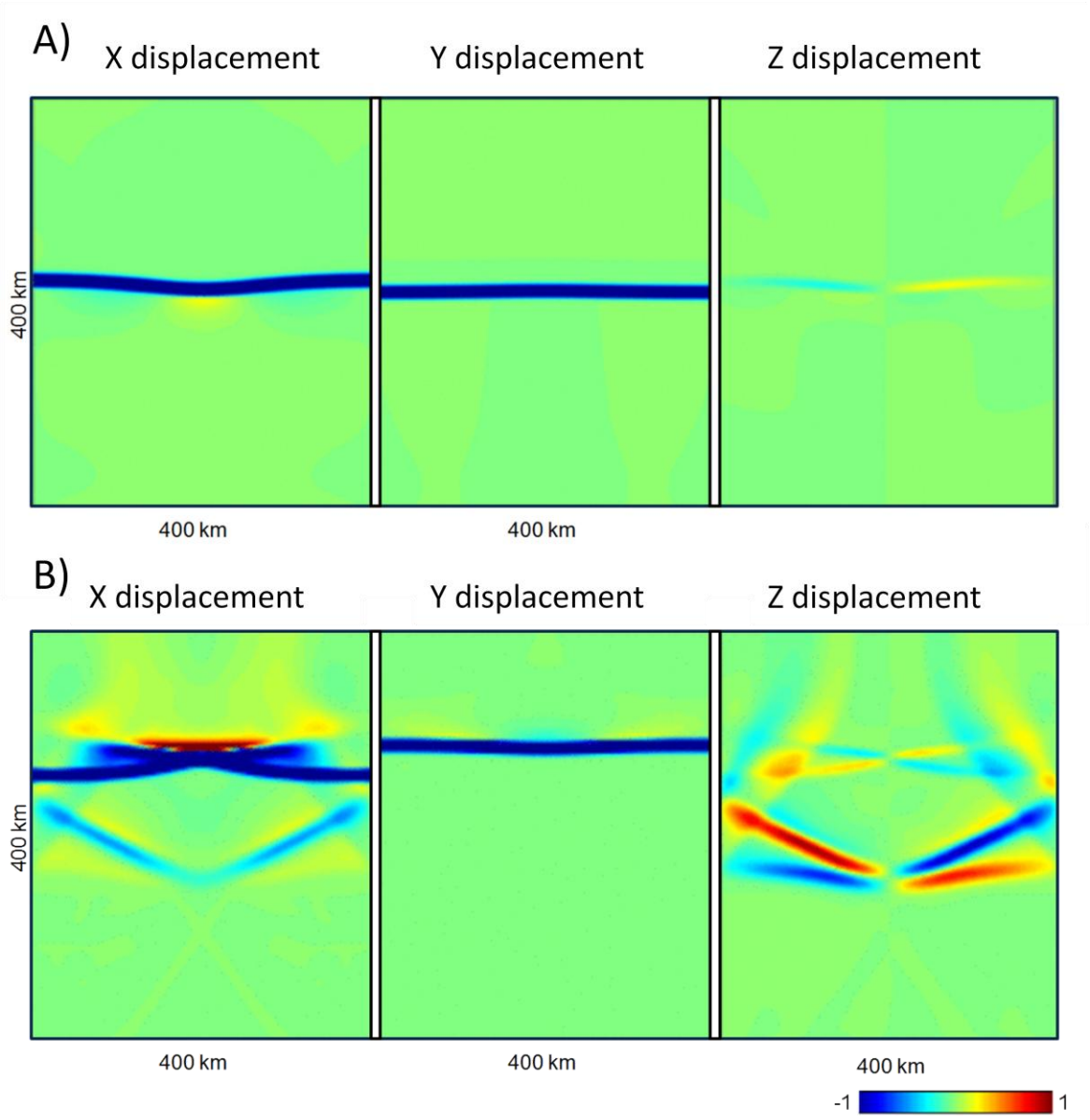

Figure 14: Time frames of the full waveform propagation through the NAA model. The figure indicates in A the wave propagation upwards whereas in B it is propagating downwards. The time frames also show the displacement for X, Y and Z direction.

It is also possible to see that the displacement in Y direction is a little late compared to the displacement in the X direction. That indicates an anisotropic medium, once both shear wave velocities have been simulated. Figure 14a is a time frame for the seismic wave propagating upwards whereas the Figure 14b is a time frame for the seismic wave propagating downwards. After the simulation of the propagations it was possible to get seismograms for all different 80 station that were set in the top of the model. As described earlier, each station is going to record three seismogram for the three directions of displacement. Using the process described in section 5.3, the shear wave splitting time was calculated for each station. The travel time was also measured and computed after simulation. In order to compare the results for full waveform propagation and for ray theory, both were plotted in Figure 15**.**

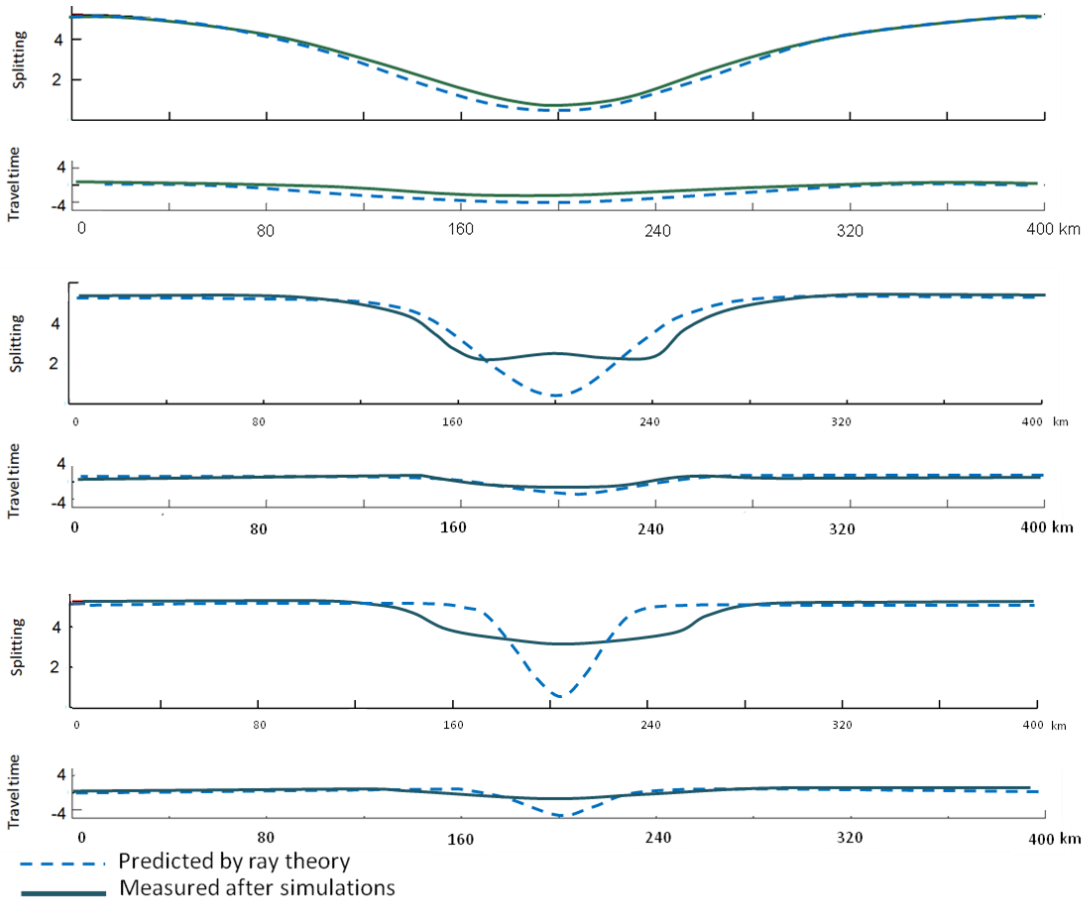

Figure 15: Splitting time and travel time profiles for anomalies of 140 km, 60 km and 30 km, respectively; both calculated after the full waveform simulation (green line) and using ray theory (blue dashed line).

7. DISCUSSIONS

Talking into account the results that are shown in Figure 15, it is clear that the width of the anomaly will affect the behavior of the wave diffraction phenomena in the full waveform simulations. The narrower the anomaly, the greater the influence of the wave diffraction in the shear wave splitting time and travel time measurements. As explained in the last sections, the full waveform simulation was run for anomalies of 140 km, 60 km and 30 km width (equivalent to parameter σ=70, σ=30 and σ=15, respectively, in the code) in order to understand how the diffraction could affect the amplitude and the shape of the shear wave splitting time anomalies once previous studies detected null splitting time measurements that could not be easily geographically related to the P and S waves anomalies generated by the NAA.

The Figure 15 shows that for a anomaly of 140 km width (σ=70), the blue and green line almost match. This shows that the wave diffraction barely affected the measurement, which means that for very wide anomalies (>140 km wide) ray theory is a good approximation for the wave propagation. For 60 km width (σ=30), the difference between the results after the simulations and the predicted one starts to be visible. Finally, for 30 km with (σ=15), the difference between them is extremely large, which suggests the wave diffraction effect is even higher. For narrow anomalies, the splitting measured by the simulation is wider, flatter and lower in amplitude than the splitting predicted by ray theory. Diffraction reduced the amplitude of the splitting delay time next to the borders of the anomaly and amplified it in the middle.

Figura 16 tries to summarize the main qualitative results of this work. It shows that for very wide anomalies, time delays and splitting time, the apparent value (what is measured

in the field) is equivalent to the expected according to the ray theory method. As the anomaly theory, the time delay and the splitting time decrease, the apparent values start to differ from the real ones, showing that ray theory starts not to be a reasonable method for wave propagation.

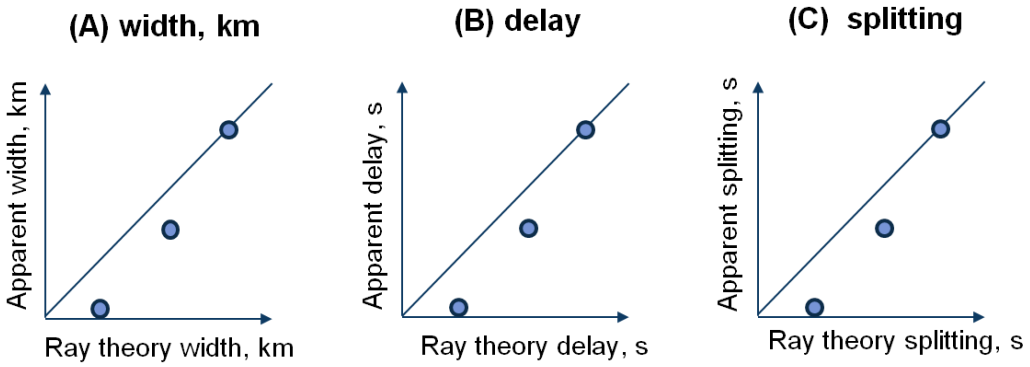

Figura 16: Summary figure showing the quality of ray theory approximations according to the increasement of the anomaly.

8. CONCLUSIONS

The object of this work was to build an anisotropic earth structure model on MATLAB that could represent the Northern Appalachian Anomaly velocity distribution; simulate a elastic anisotropic full waveform propagation in it; and to measure the shear wave splitting time profile along the earth structure model in order to understand if the wave diffraction phenomena would be able to affect the results.

We understand that the simulation used in this paper is based on elastic wave equation, which is more realistic than the ray theory results because it considers the wave diffraction effect. That is why in the previous sections both results are compared. Once all of these processes were done it was possible to verify that the wave diffraction phenomena is able to affect not only the splitting measurements but also the time delay results. It was also verified that this influence depends on the width of the anomaly.

After the comparison between ray theory and the simulation results it was concluded that the minimum width for an anomaly to affect the splitting measurements is equal to 60 km whereas for very wide anomalies (>140 km wide) ray theory is a good approximation for the wave propagation.

Once the width of the NAA is about 400 km and the minimum width for an anomaly to affect the splitting measurements is about 60 km the wave diffraction phenomena does not explain the null splitting time in the NAA anomaly region. In order to try to explain the distribution of null shear wave splitting times in New England it is necessary to invest in new works such as this one, in which it was able to study the limitation of the methods used to image the Northern Appalachian Anomaly.

9. REFERENCES

ANDO, M. (1984). ScS polarization anisotropy around the Pacific Ocean, J. Phys. Earth, 32, 179-196.

BACKUS GE. 1962. Long-wave elastic anisotropy produced by horizontal layering. *J. Geophys. Res.* 67:4427–40.

BARTHOLOMEW, M.J., and WHITAKER, A.E., 2010, The Alleghanian deformational sequence at the foreland junction of the Central and Southern Appalachians *in* Tollo, R.P., Bartholomew, M.J., Hibbard, J.P., and Karabinos, P.M., eds., From Rodinia to Pangea: The Lithotectonic Record of the Appalachian Region, GSA Memoir 206, p. 431-454.

BOYD, O. (2006). *An efficient Matlab script to calculate heterogeneous anisotropically elastic wave propagation in three dimensions*. Elsevier, 259-264. doi:10.1016/j.cageo.2005.06.019

CHRISTENSEN N.I. (1984). The magnitude, symmetry and origin of upper mantle anisotropy based on fabric analyses of ultramafic tectonics. *Geophys. J. R. Astron. Soc.*

76:89–112

CRAMPIN S., BOOTH D.C. (1985). Shear-wave polarizations near the North Anatolian Fault, II, Interpretation in terms of crack-induced anisotropy. *Geophys. J. R. Astron. Soc.* 83:75– 9

EATON, D., & FREDERIKSEN, A. (2007). Seismic evidence for convection-driven motion of the North American plate. *Nature,* 428-431. doi:10.1038/nature05675.

GAHERTY J.B., JORDAN T.H. 1995. Lehmann Discontinuity as the base of an anisotropic layer beneath continents. *Science* 268:1468–71.

HYNES, A., & RIVERS, T. (2010). Protracted continental collision — evidence from the Grenville Orogen. *Canadian Journal of Earth Sciences*,*47*(5), 591-620. doi:10.1139/E10-003.

KANESHIMA S., ANDO M. 1989. An analysis of split shear waves observed above crustal and uppermost mantle earthquakes beneath Shikoku, Japan: implications in effective depth extent of seismic anisotropy. *J. Geophys. Res.* 94:14,077–92.

KANESHIMA S., ANDO M., KIMURA S. 1988. Evidence from shearwave splitting for the restriction of seismic anisotropy to the upper crust. *Nature* 335:627–29

KING, S. D., and RITSEMA, J. (2000), African hot spot volcanism: Small-scale convection in the upper mantle beneath cratons, Science, 10, 1137–1140, doi:10.1126/science.290.5494.1137.

LAY, T. (1995). *Modern Global Seismology* (T. Wallace & T. Lay, Eds.). Academic Press.

LEVIN, V., LERNER-LAM, A. and W. MENKE, W. (1995), Anomalous mantle structure at the Proterozoic-Paleozoic boundary in northeasten US, Geophys. Res. Lett., 22, 121–124, doi:10.1029/94GL02693.

LI, A., K.M. FISHER, M.E. Wysession and TJ. Clarke, *Mantle discontinuities and temperature under the North American continental keel*, Nature 395, 160-163, doi:

10.1038/25972, 1998.

LONG, M. D., K. G. JACKSON, and J. F. McNAMARA (2016), SKS splitting beneath Transportable Array stations in eastern North America and the signature of past lithospheric deformation, Geochem. Geophys. Geosyst., 17, 2–15, doi:10.1002/ 2015GC006088.

McKENZIE D. 1979. Washington, DC: Am. Geophys. Union Finite deformation during fluid flow. *Geophys. J. R. Astron. Soc.* 58:689– 715 Ribe NM. 1989a. A continuum theory for lattice preferred orientation. *Geophys. J. Int.* 97:199–207

McNAMARA D.E. 1990. *Evidence for azimuthal seismic anisotropy in the Basin and Range Province: implications for middle to lower crustal tectonic processes.* MS thesis. Univ. Missouri, Columbia. 125 pp.

McNAMARA DE, OWENS T.J. 1993. Azimuthal shear wave velocity anisotropy in the Basin and Range Province using Moho Ps converted phases. *J. Geophys. Res.* 98:12,003–17

MENKE, W., P. SKRYZALIN, V. LEVIN, T. HARPER, F. DARBYSHIRE, and T. DONG (2016), The Northern Appalachian Anomaly: A modern asthenospheric upwelling, Geophys. Res. Lett., 43, 10,173–10,179, doi:10.1002/ 2016GL070918.

NATAF H.C., NAKANISHI I., ANDERSON D.L. 1984. Anisotropy and shear-velocity heterogeneities in the upper mantle. *Geophys. Res. Lett.* 11:109–12

NICOLAS A., CHRISTENSEN N.I. 1987. Formation of anisotropy in upper mantle peridotites—A review. In *Composition, Structure and Dynamics of the Lithosphere-Asthenosphere System,* ed. K Fuchs, C Froidevaux, 16:111–23.

NICOLAS A., POIRIER J.P. 1976. *Crystalline Plasticity and Solid State Flow in Metamorphic Rocks.* New York: Wiley. 444 pp.

RIBE N.M. 1989b. Seismic anisotropy and mantle flow. *J. Geophys. Res.* 94:4213–23.

RIBE NM,YuY. 1991.Atheory for plastic deformation and textural evolution of olivine polycrystals. *J. Geophys. Res.* 96:8325–35.

SAVAGE M.K., SHIH X.R., MEYER R.P., ASTER R.C. 1989. Shear-wave anisotropy of active tectonic regions via automated S-wave polarization analysis. *Tectonophysics* 165:279–92.

SCHMANDT, B., and F.-C. LIN (2014), P and S wave tomography of the mantle beneath the United States, Geophys. Res. Lett., 41, doi:10.1002/2014GL061231.

SCHLUE, J., & L. KNOPOFF, L. (1977). Shear-wave polarization anisotropy in the

Pacific Basin. *49*(1), 145-165. doi:10.1111/j.1365-246X.1977.tb03706.x.

SHEARER, P. (2009). *Introduction to Seismology* (2nd ed.). New York, NY: Cambridge University Press.

SHEARER, P.M., 1999. The seismic wave equation. In: Shearer, P.M. (Ed.), Introduction to Seismology. Cambridge University Press, Cambridge, pp. 25–34.

SILVER, P. (1996). Seismic Anisotropy beneath the continents: Probing the Depths of Geology. *Annual Review of Earth and Planetary Sciences,24*, 385-432. doi:10.1146/annurev.earth.24.1.385

VAN DER LEE, S., & Nolet, G. (1997). Upper mantle S velocity structure of North America. *Journal of Geophysical Research,102*(10), 22, 815-22, 838. doi:10.1029/97JB01168.

WALDHAUSER, F., LIPPITSCH, R., KISSLING, E., & ANSORGE, J. (2002). High-resolution teleseismic tomography of upper-mantle structure using an a priori three-dimensional crustal model. *Geophysical Journal International, 150*, 403-414.